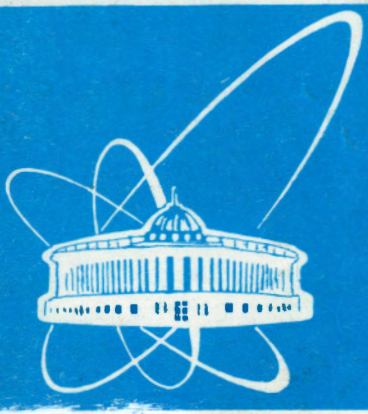

объединенный
институт
ядерных
исследований
дубна

E7-94-381

ON THE TIME SCALE OF MULTIFRAGMENT EMISSION IN ^{4}He+Au COLLISIONS AT E/A = 3.65 GeV/NUCLEON

Submitted to «Ядерная физика»

1994

S.Y.Shmakov, S.P.Avdeyev, V.A.Karnaukhov, V.D.Kuznetsov, L.A.Petrov, E.A.Cherepanov
Joint Institute for Nuclear Research, 141980 Dubna, Moscow Region, Russia

V.Lips, R.Barth, H.Oeschler
Institut für Kernphysik, Technische Hochschule Darmstadt, 64289 Darmstadt, Germany

A.S.Botvina
Institute of Nuclear Research, P.O.Box 117312, Moscow, Russia

O.V.Bochkarev, L.V.Chulkov, E.A.Kuzmin
Kurchatov Institute, P.O.Box 123182 Moscow, Russia

W.Karcz
Henryk Niewodniczanski Institute of Nuclear Physics, 31-342 Cracow, Poland

W.Neubert
Institut für Kern- und Hadronenphysik, Forchungszentrum Rossendorf, 01314 Dresden, Germany

E.Norbeck
University of Iowa, Iowa City, IA 52242 USA

1. Introduction

Nuclear multifragmentation has been of great experimental and theoretical interest in the last years. The mechanism of this decay mode is not clear yet. A still open question is whether the emission of intermediate mass fragments (IMF, $3 \leq Z \leq 20$) can be understood by evaporation-like process [1,2], or it is a new phenomenon of hot and diluted nuclear matter, where the emission occurs within very short time. This "simultaneous break-up" mechanism has been associated with volume instabilities [3,4], which are related to a liquid–gas phase transition in nuclear matter [5], or with surface instabilities which can arise, if a system attains some unusual shapes [6,7].

The experimental studies of multifragment emission have been conducted in the last years mainly by means of heavy ion beams. The recent reviews on the problem are given in [8,9].

The time scale of the IMF emission is a very important characteristic for understanding of the multifragmentation phenomenon. In a number of previous experiments it was derived from the IMF–IMF relative velocity correlation function which exhibits a minimum at $v_{rel} = 0$ originating from repulsive Coulomb final state interaction between emitted fragments.

One should have in mind that two different parametrizations of the multifragmentation time scale are used. In the first one the time scale is characterized by the mean lifetime τ of the fragmenting system, and the emission times are randomly distributed according to the exponential law $P(t) \sim \exp(-t/\tau)$ [10,11,12]. The average time interval between subsequent emissions of the fragments depends on the mean IMF-multiplicity: $< \Delta t >= \tau* = \frac{\tau}{M-1} \sum_{n=1}^{M-1} \frac{1}{n}$. Slightly different parametrization is used in ref. [13,14]: the time delays between subsequently emitted fragments are characterized by an exponential probability distribution: $P(\Delta t) \sim \exp(-\Delta t/\tau*)$. The mean emission time $\tau < 100$ fm/c was deduced for central ^{36}Ar+Au collisions at E/A = 50 - 100 MeV by means of the three body Coulomb trajectory model [10]. A larger limit (250 fm/c) was obtained for ^{56}Fe+Au collisions at E/A = 100 MeV [13]. In ref. [14] it was concluded that for Kr+Nb collisions the mean delay time between fragments decreases from 400 fm/c at E/A = 35 MeV to 125 fm/c at E/A = 55 MeV with possible saturation at higher energies. The evidence for very short values of τ was obtained from measurements with a 600 MeV/u gold beam and different targets in inverse kinematics [15].

In a paper by the collaboration FASA [12] the time scale for the multifragment decay is estimated for a very asymmetric system ^{4}He+Au at 3.65 GeV/n. Compared to the above-mentioned experiments, this very asymmetric system has several advantages: (i) All detected IMF's are emitted from the target spectator and there is no mixture of different sources like in heavy ion reactions. (ii) One should expect that with ^{4}He–projectiles dynamic effects are small, the compression of the target nucleus in collision is negligible. One should expect that in this case decay of the excited target spectator proceeds in an apparently statistical manner ("thermal multifragmentation"). To extract the time scale the analysis of IMF–IMF correlation in respect to the relative angle was performed like in ref. [11]. The relative angle distribution exhibits a minimum at $\Theta_{rel} = 0$ arising from the Coulomb repulsion between fragments. A magnitude of this effect drastically depends on the time scale of

the emission, since the longer time distance between fragments the larger their space separation and hence the weaker their Coulomb repulsion. By multi-body Coulomb trajectory calculation it was shown that the mean lifetime of the source is less than 100 fm/c. The initial configuration for these calculations — IMF masses and charges, their start positions and velocities — were calculated in the framework of the statistical fragmentation model of Gross [16]. It is obvious that such indirect estimation of the time scale may be model-dependent.

Having this in mind, in present paper we performed an analysis of the relative angle distribution between IMF's using another code for multi-body Coulomb trajectory calculations and the Copenhagen-Moscow statistical fragmentation model [17]. These calculations also give evidence for fast break-up of target-spectator in the reactions induced by relativistic ^{4}He-projectiles.

2. Data sampling

The experiment was performed with a 4π-setup FASA [18], installed at the external beam of the JINR-synchrophasotron. The main parts of the device are the following: (i) an IMF multiplicity detector (FMD), consisting of 55 thin (50 μm) CsJ(Tl) counters, which cover the main part of 4π; (ii) five time-of-flight telescopes, which measure energies, velocities and masses of IMF's at selected angles (50°, 68°, 94°, 103°, 117°). They serve as a trigger for the read-out of the system; (iii) a large position-sensitive parallel-plate avalanche counter (PPAC), which allows one to determine the relative angle and velocity correlations of fragments detected in coincidence with TOF's in the angular range $\Theta_{rel} = 15 - 180°$. Whereas the TOF's efficiency does not constrain the registration of fragments with A$\geq$6, the PPAC reaches full detection efficiency only for IMF's with Z>5. That has been taken into account in all calculations presented later on.

A self-supporting Au target 1.0 mg/cm^2 thick was irradiated by a 3.65 GeV/u ^{4}He beam at intensity $5 \cdot 10^8$/spill.

The TOF telescope covers only a small solid angle ($\sim 10^{-3}$sr.). Therefore the triggering probability is proportional to the multiplicity in the event. Going from peripheral collisions to the central ones, one should expect an increase in the target-spectator excitation energy as well as IMF multiplicity. So our trigger conditions suppress the contribution of the peripheral collisions and enhance the detection of more hard collisions. It is demonstrated in ref. [19], where it is shown that the IMF multiplicity distribution being shaped like a Fermi function becomes Poisson-like when trigger conditions are applied.

3. Description of the model

The interaction of ^{4}He projectiles with the Au target proceeds through three stages. The initial fast stage is described by the intranuclear cascade model [20]. Intranuclear cascades cease by forming excited residual nuclei with charges (Z_R), masses (A_R) and excitation energies (E_R), distributed over wide ranges depending on the impact parameter of the collisions. Some of them, if the excitation energy is high enough, undergo multiple emission of fragments. The mean values for residual nuclei decaying by emission of at least two IMF's are the following: $< Z_R > = 62$,

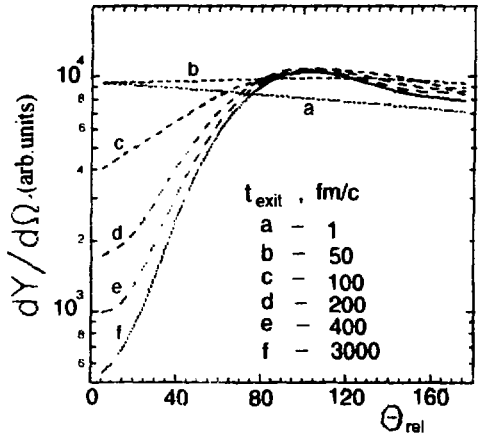

Fig. 1. Distributions of relative angles between coincident fragments at different times t_{exit} after the break-up moment.

$< A_R > = 155, < E_R > = 1250$ MeV. This second stage of the reaction is described by the statistical multifragmentation model [17]. Within this model the probabilities of different decay channels are proportional to their statistical weights. The break-up volume determining the Coulomb energy of the system is taken as $V_b = (1+k)\, A_R/\rho_o$, where $\rho_o = 0.15$ fm^{-3} is the equilibrium nuclear density and k is a model parameter. So, the thermal expansion of the system before the break-up is assumed.

The primary fragments are hot. At the final stage deexcitation of hot fragments leads to formation of ensembles of cold fragments, which can be detected. All the stages of the reaction are simulated by the Monte Carlo method, so the characteristics of all particles produced in a single event are calculated.

The statistical multifragmentation model gives the positions and momenta of all the fragments and they are used in the further calculations. Classical Coulomb trajectories of all the charged particles in the event are calculated by a code developed in ref. [21]. First of all evolution of the trajectories during the acceleration was investigated. Fig. 1 presents the distributions of the relative angles between momenta of fragments for each pair in the event at different time t_{exit} after the start of the acceleration. These calculations are made for prompt break-up of the system and $k = 2$ ($\rho_b = \frac{1}{3}\rho_o$). Secondary disintegration of the hot fragments was included after acceleration, and selection according to the experimental filter was performed. At the initial moment there is some enhancement at small angles, caused by the recoil momentum of the residual nucleus. The "Coulomb minimum" develops between 50 and 1000 fm/c after the break-up moment. So, 3000 fm/c is the proper time to stop the trajectory calculations. Kinetic energy at this moment is very close to the asymptotic value. It is clear from Fig. 2, where the mean kinetic energy of the fragment (Z = 6÷7) and the depth of Coulomb minimum are shown as a function of the acceleration time. As a measure of the Coulomb repulsion effect, we use the ratio of the coincidence counting rates for $\Theta_{rel} = 25°$ and $\Theta_{rel} = 100°$.

Fig. 3 shows how this effect depends on the mean lifetime of the fragmenting system if one selects IMF with $12 < A \leq 30$. One can estimate from Fig. 3 that the accuracy of τ determination (90% CL) is ~(20–40) fm/c for $\tau \leq 200$ fm/c and 10% of counting statistics at $\Theta_{rel} = 25°$.

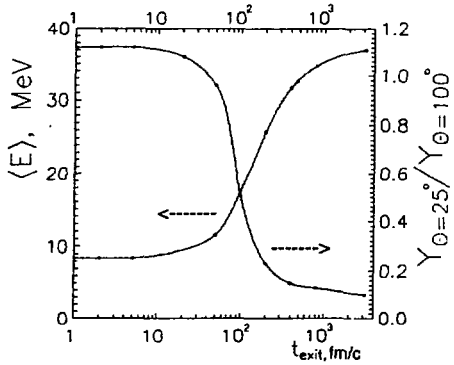

Fig. 2. The mean kinetic energy of a fragment (Z = 6÷7) and the magnitude of the small angle suppression as a function of the acceleration time.

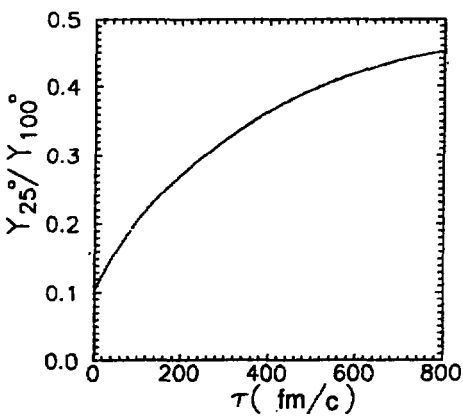

Fig. 3. The magnitude of the small relative angle suppression as a function of the mean lifetime of the fragmenting system.

4. Comparison between model and experimental data

Fig. 4 presents the experimental data on relative angle distribution for coincident fragments detected by TOF telescopes and large position-sensitive PPAC. Two ranges for masses of fragments detected by TOF have been chosen: $6 \leq A_{TOF} \leq 12$ and $12 < A_{TOF} \leq 30$. Suppression of small angles is larger for the second case because of stronger Coulomb interaction between fragments. Theoretical curves in Fig. 4a have been obtained for the prompt multifragment decay of the system with break-up density $\rho_b = \frac{1}{3}\rho_o$. They describe the experimental data rather well especially for the second mass interval.

To check the sensitivity of the relative angle distribution to the freeze-out density the calculations were done with k = 7 ($\rho_b = \frac{1}{8}\rho_o$). The results are presented in Fig. 4c. The sensitivity is rather weak. This allows adjustment of this parameter by using relative velocities of coincident fragments at large correlation angles, which crucially depend on the source size. The experimental mean value of the relative velocity for $\Theta_{rel} > 150°$ is equal to 3.77±0.02 cm/ns [19]. The calculated values in this model are equal to 3.76 cm/ns for k = 2 and 3.33 cm/ns for k = 7. So for further analysis the break-up density was chosen to be $\frac{1}{3}\rho_o$.

In this calculation the break-up of hot fragments before detection was included in contrast to the previous paper of our collaboration [12]. The effect of the secondary disintegration is seen in Fig. 4b, where the result of the calculation without this stage of the reaction is shown. Secondary fragmentation results in slightly diminishing suppression of small relative angles because of additional recoil momentum. This is a reason why calculations presented here give a little bit weaker effect of suppression of small relative angles in comparison to ref. [12].

The calculations assumed a time delay between successively emitted fragments were performed with the same initial configurations as in the case of the prompt break-up. The emission times were randomly distributed following the exponential decay law $P(t) \sim \exp(-t/\tau)$, where τ is the mean lifetime of the fragmenting source. Fig. 5 shows the experimental data and calculated results for relative angle distribution for coincident fragments. To improve statistical accuracy the full mass range of IMF's, detected by TOF telescopes, was taken ($6 \leq A_{TOF} \leq 30$). Calculations were made for τ-values equal to 0, 100, 400 and 800 fm/c. The best fit corresponds to the prompt decay. The point at 25° deviates from the theoretical curve for $\tau = 100$ fm/c by more than 3 standard deviations. So we conclude that the mean lifetime of the fragmenting system is definitely less than 100 fm/c and the mean separation time between two successively emitted IMF's is less than 50 fm/c (for mean IMF multiplicity equal to 5). This conclusion completely coincides with that in our previous paper [12].

The results presented here support a scenario of true thermal multifragmentation with the so-called simultaneous emission of fragments. There are not absolutely prompt processes, any one has a definite width or time scale. In the case of multifragmentation it is determined by characteristic time for density fluctuations, which lead to the fragment formation. A number of the papers were devoted to the theoretical estimation of the rate of fragment formation by both the thermodynamical model [22] and the quantum molecular dynamic approach [23-25]. The mean emission time is predicted to be (50-100) fm/c in agreement with both the experimental data for

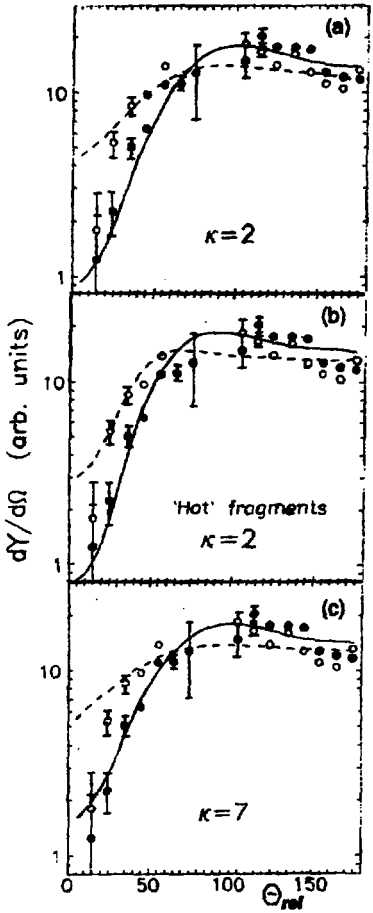

Fig. 4. Distribution of the relative angles between two IMF's for different mass ranges of the fragments detected in the TOF. Open and full circles are experimental data for $6 \leq A_{TOF} \leq 12$ and $12 < A_{TOF} \leq 30$ respectively. Dashed and solid lines are results of calculations for simultaneous emission of fragments in these two ranges of A_{TOF}.

a) Break-up density is $\frac{1}{3}\rho_o$ with the secondary decay of a fragment after acceleration.

b) The same as a) but the secondary decay is not included.

c) Break-up density is $\frac{1}{8}\rho_o$.

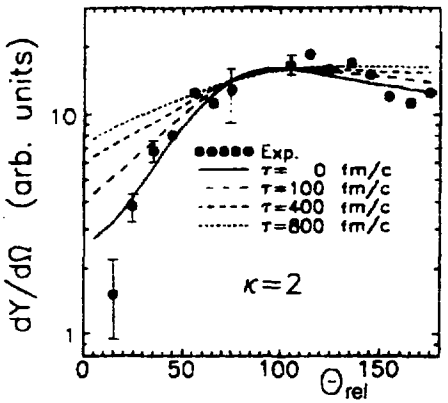

Fig. 5. Distribution of relative angles between IMF's; $6 \leq A_{TOF} \leq 30$. The curves are calculated for 4 values of the mean lifetime τ of the fragmenting system. Error bars are shown where they exceed the point size.

heavy-ion induced multifragmentation and the data presented here. The statistical model of the sequential evaporation of fragments also gives rather short emission time ($\tau \simeq 100$ fm/c), considering the decay of very hot ($T \geq 13$ MeV) and expanding nucleus [26]. So, one could hardly distinguish between "simultaneous" break-up and sequential evaporation if the time scales of both processes are really close to each other.

5. Conclusions

The distribution of relative angles between intermediate mass fragments has been measured and analyzed on the event-by-event basis for the target-spectator fragmentation in ^{4}He+Au collisions at 3.65 GeV/nucleon. It was shown that the yield of fragment pairs with small relative angles is suppressed because of Coulomb repulsion between fragments. This effect is very sensitive to the time delay between successively emitted fragments. The multi-body Coulomb trajectory calculations have been performed starting from the initial break-up conditions as given by the combined model with an intra-nuclear cascade followed by statistical multifragmentation of the residual nucleus. The mean lifetime of a fragmenting system $\tau \leq 100$ fm/c was estimated from comparison of the calculated relative angle distribution with the experimental one. The present result on the fragment emission time scale supports a scenario of true "thermal" multifragmentation of an expanded nuclear system.

We would like to thank Profs A.M. Baldin, S.T. Belyaev, A. Budzanowski, A. Hrynkiewicz, E. Kankeleit and A.N. Sissakian for support. This work is supported in part by the Russian Fundamental Research Foundation under project No.93-02-3755, the International Science Foundation under Grant No.RFK000, the Bundesministerium für Forschung und Technologie under contract No.06DA453.

References

1. L.C. Moretto and G.J.Wozniak, *Progr. Part and Nucl. Phys.* 1988. V. 60. P. 2195.
2. W. Friedman, *Phys. Rev.*, 1990. V. C42. P.667.
3. J. Bondorf, R. Donangelo, I.N. Mishustin, H. Schulz, *Nucl. Phys.* 1985. V. A444. P. 460.
4. D.H.E. Gross, *Nucl. Phys.* 1985. V. A437. P. 313c.
5. P.J. Siemens, *Nature.* 1983. V. 305. P. 410;
   A.D. Panagiotou, M.W. Curtin, D.K. Scott, *Phys. Rev.* 1985. V. C31. P. 55.
6. L.G. Moretto et al. *Phys. Rev. Lett.* 1992. V. 69. P. 1884.
7. W. Bauer, G.F. Bertsch, H. Schulz, *Phys. Rev. Lett.* 1992. V. 69. P. 1888.
8. L.G. Moretto, G.J. Wozniak, *Ann. Rev. Nucl. Part. Sci.* 1993. V. 43. P. 379.
9. Proc. of Int. Workshop XXII on Gross Properies of Nuclei and Nucl. Excitations-Multifragmentation, Hirschegg, Austria (1994), ed. by H. Feldmeier and W. Nörenberg, GSI, Darmstadt.
10. D. Fox, et al. *Phys.Rev.* 1993. V. C47. P. R421.
11. M. Louvel, et al. *Phys. Lett.* 1994. V. B320. P. 221.
12. V. Lips, et al. *Phys. Lett.* (in print).
13. T.C. Sangster, et al. *Phys. Rev.* 1993. V. C47. P.R2457.
14. E. Bauge, et al. *Phys. Rev. Lett.* 1993. V. 70. P. 3705.
15. V. Lindenstruth, et al. *Preprint GSI*-93-54, Darmstadt, 1993.
16. D.H.E. Gross, *Rep. Progr. Phys.* 1990. V. 53. P. 605.
17. A.S. Botvina, A.S. Iljinov, I. Mishustin, *Nucl. Phys.* 1990. V. A507. P. 649.
18. S.P. Avdeyev, et al., *Nucl. Instr. Meth.* 1993. V. A332. P. 149.
19. V. Lips, et al., *Phys. Rev. Lett.* 1993. V. 72. P. 1604.
20. V.D. Toneev, K.K. Gudima, *Nucl. Phys.* 1983. V. A400. P. 173C.
21. P.G. Akishin, et al., JINR, E11-94140, Dubna, 1994.
22. R. Donangelo, K. Sneppen, J.P. Bondorf, *Phys. Lett.* 1989. V. B219. P. 165.
23. D.H. Boal and J.N. Glosli, *Phys. Rev.* 1988. V. C37. P. 91.
24. G. Peilert, et al., *Phys. Rev.* 1989. V.C37. P. 1402.
25. J. Bondorf, A.S. Botvina, I.N. Mishustin, S.R. DeSouza, *Phys. Lett.* (in print)
26. W. Friedman, Proc. of Int. Symp. "Towards a Unified Picture of Nucl. Dynamics", Nikko Japan, ed. by Y. Abe, S. Lee and F. Sakata, AIP Conf. Proc. No 250 (N.Y. 1992) P.422.

Received by Publishing Department
on September 28, 1994.